Resonating-valence-bond physics and topological order in two dimensions: from dimer models to high-temperature superconductivity

Dmitri A. Ivanov

Institute of Theoretical Physics, Ecole Polytechnique Fédérale de Lausanne (EPFL), CH-1015 Lausanne, Switzerland

Abstract. The notion of Z_2 topological order in two-dimensional resonating-valence-bond systems is reviewed. Using quantum dimer models as an example, I discuss general properties of the topological order and the resulting vortex-like excitations (visons). Some connections to theories of frustrated magnetism and of high-temperature superconductivity are pointed out.

Keywords: resonating-valence-bond state, quantum dimer models, high-temperature superconductivity, topological order
PACS: 74.20.Mn, 75.10.Jm, 03.75.Lm, 71.10.Fd

RESONATING-VALENCE-BOND STATE

The idea of a quantum spin liquid, i.e., a spin system which does not order in any way down to zero temperature (in two or three dimensions), has been an important topic of research in condensed-matter physics since many years. Under certain conditions, such a state would imply a novel strongly correlated phase of matter with unusual low-temperature properties [1], and it has been sought for both theoretically and experimentally. Obvious candidates for a quantum liquid phase are so-called frustrated spin systems, where the signs of interactions between the spins disfavor any sort of magnetic ordering. On the other hand, spin-liquid physics has also been proposed to be relevant for high-temperature superconductivity, where magnetic order is destroyed by the doped holes [2]. By now, many theories and models have been constructed for spin liquids [3, 4, 5, 6, 7, 8] and some experiments (e.g., on the herbertsmithite $ZnCu_3(OH)_6Cl_2$ [9]) seem to indicate a possible spin-liquid state. Nevertheless, up to date, there has been no rigorous argument for a stable spin-liquid state in a realistic spin model.

The most popular spin-liquid scenario is the so-called resonating-valence-bond (RVB) state, which has been proposed for spin-1/2 systems in the two-dimensional geometry [10], and which has soon found its application also in the theory of high-temperature superconductors [2]. Since then, the development of the RVB theory continued in two parallel lines (with mutual influence): RVB physics in spin systems and in dimer models on one side, and the RVB scenario of high-temperature superconductivity on the other side.

RVB state in spin and dimer systems

In analyzing low-temperature phases of frustrated magnets, it has soon been realized that spins usually tend to order either magnetically or as a crystal of singlets. The RVB-liquid phase of frustrated magnets has mostly been suggested numerically, without a solid analytic support (see, e.g., Ref. [11] for a review). A more rigorous and controllable way to realize the RVB phase is to consider quantum dimer models or other models with an explicit Z_2 gauge symmetry [12]. One of the simplest and most convenient systems for studying the RVB phase is the Rokhsar–Kivelson (RK) dimer model [13]. If formulated on the square lattice, it only has the RVB phase at one point in the space of parameters (corresponding to a transition between two crystal phases). The excitation spectrum is gapless at this point, which is a consequence of a conserved "winding number" for dimer models on bipartite lattices [14, 15]. On the triangular lattice, however, there is a finite region of parameters where the RVB phase is stable with a finite energy gap [16].

While properties of the RVB state in dimer models are quite well understood (see the sections below), finding a realistic spin model with a confirmed RVB state remains a challenging theoretical problem.

RVB state in high-temperature superconductors

In application to high-T_c superconductivity, the RVB physics appears in the Gutzwiller-projected construction of variational wave functions [2]. After the first systematic application of this method [17], a variety of

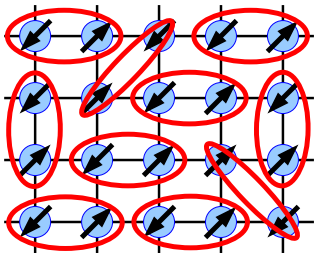

FIGURE 1. A schematic view of a RVB state. The electrons form short-range singlets. The RVB state is a linear combination of various singlet configurations that preserves all the lattice symmetries.

works have appeared analyzing low-temperature properties of the t–J model (a generic model for high-T_c superconductors) with the use of variational wave functions [18, 19, 20]. Those predictions, even for the simplest version of the model with only nearest-neighbor hopping and with the only parameter $t/J = 3$ appear to be qualitatively consistent with the commonly observed properties of cuprates [21]. The low-temperature phases include a d-wave superconductor [17] with an antiferromagnetic instability at very low doping [19], in agreement with the experimental phase diagram. Recently, more detailed studies have appeared with computations of such quantities as condensation energy, superfluid density, coherence length, quasiparticle spectral weight, Fermi velocity, etc [22, 23, 24, 25].

Z_2 TOPOLOGICAL ORDER AND VORTEXLIKE EXCITATIONS (VISONS)

The RVB state is usually defined in the following way: the spins are grouped into singlet pairs, and the ground state is a linear combination of various singlet configurations (Fig. 1).

Such a state is conjectured to have a Z_2 topological order [26], and its elementary excitations are spin-1/2 spinons and Z_2 vortices (visons) [27, 28]. The topological order and the vortexlike excitations remain at the level of conjecture for spin systems, but can be rigorously proven and studied for a simpler type of systems: dimer models.

Topological order

In dimer models, the spin singlets are replaced by unbreakable dimers (Fig. 2), and different dimer configurations are orthogonal by definition. Then a new type of conservation law emerges: for any closed contour, any *local* rearrangement of dimers does not change the *parity*

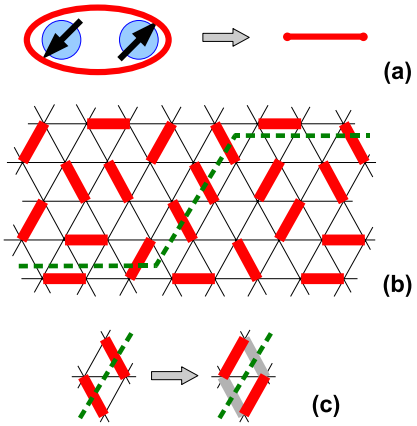

FIGURE 2. Dimer models. **(a)**: Replacing singlets by dimers. The overlap between different dimer configurations is zero by definition, unlike for singlets. **(b)**: An example of a dimer configuration. For any (closed) contour, the parity of the number of intersections with dimers is invariant with respect to local dimer rearrangement. **(c)**: An example of a local dimer rearrangement. This elementary rearrangement of two dimers constitutes the kinetic term in the Rokhsar–Kivelson dimer model (1).

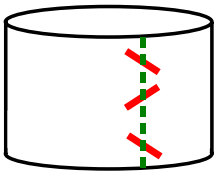

FIGURE 3. For a cylinder, one chooses a contour connecting the two edges. The parity of dimer intersections with this contour distinguishes the two topological sectors: even and odd.

of the number of intersecting dimers (Z_2 index of intersection) (Fig. 2) [27, 28]. Note that this conservation law does not depend neither on the geometry of the lattice nor on the type of local rearrangement. For bipartite lattices, an additional conservation law appears, which extends the symmetry from Z_2 to $U(1)$ [14, 15]. In this paper, I assume that the lattice of available dimer positions is not bipartite, and therefore I will not consider the $U(1)$ case.

This conservation law leads to the existence of *topological sectors* for systems defined on multiply connected domains (cylinder, torus, plane with holes, etc.): the Hilbert space splits into several disconnected components. Assuming the *absence of dimer crystallization* (all correlations are exponentially decaying), this further leads to a topological degeneracy in the thermodynamic limit (as the system size L tends to infinity) (Fig. 3).

In general, the notion of Z_2 topological order in RVB-type systems may be formulated in the form of *two conditions* [29, 30]: on a multiply connected domain, the

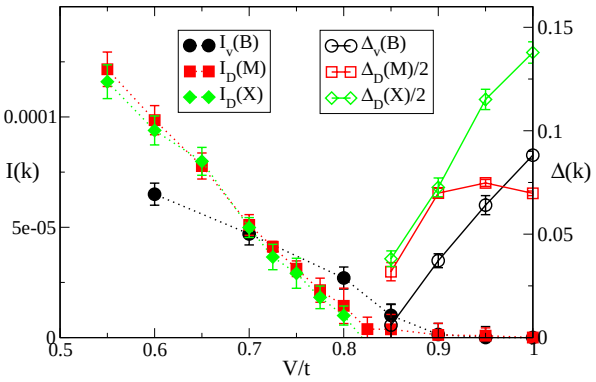

FIGURE 4. A numerical evidence for the second-order crystallization transition in the RK dimer model. Solid squares and diamonds represent the dimer Bragg peaks at two different points in the Brillouin zone. Solid circles represent the vison Bragg peaks (multiplied by 0.01, to be shown on the same scale). Open circles represent the vison gap, and open squares and diamonds represent the dimer gaps at the two points in the Brillouin zone. The horizontal axis is the ratio v/t in the Hamiltonian (1). From Ref. [35].

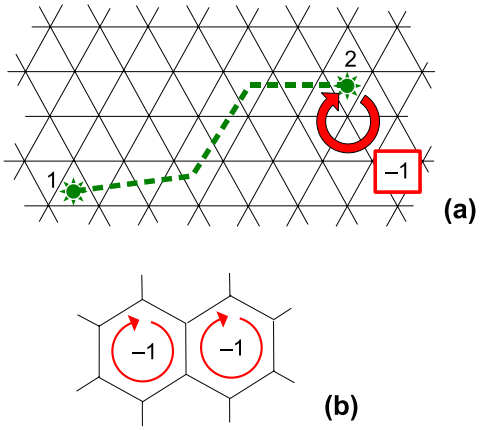

FIGURE 5. **(a)**: The point-like visons V_i are defined on the dual lattice with frustration. **(b)**: For the triangular lattice, the dual lattice is hexagonal. The frustration may be represented by the magnetic field of half flux quantum per plaquette

degenerate ground states $|A\rangle$ and $|B\rangle$ should obey:

1. identical local properties: $\langle A|X|A\rangle = \langle B|X|B\rangle$ in the limit $L \to \infty$ for any local operator X;
2. orthogonality: $\langle A|X|B\rangle$, again, in the thermodynamic limit $L \to \infty$ for any local operator X.

Note that the second condition is automatically satisfied for dimer models, while the first condition amounts to the absence of dimer crystallization. In spin systems, the second condition becomes also nontrivial and can be approximately related to the absence of spin ordering [30].

Topological order in the RK dimer model

A typical example of the system with the Z_2 topological order described above is the Rokhsar–Kivelson dimer model on the triangular lattice [4, 31]. For dimers on the triangular lattice, the quantum dynamics is defined by the Hamiltonian:

$$H_{\rm RK} = \sum \Big(-t\, |\, \rangle\langle\, | + v\, |\, \rangle\langle\, | \Big) \qquad (1)$$

where the sum is performed over all rhombi containing two parallel dimers. The kinetic term with the coefficient t flips the pair of dimers as shown in the bottom panel of Fig. 2, while the potential term with the coefficient v assigns a potential energy to such pairs of dimers.

For the special case $v = t$ (the "Rokhsar–Kivelson point"), the RVB phase is rigorously proven, with the exponential decay of correlation functions and with the two conditions of the topological order (formulated above) satisfied [32, 31]. An extensive numerical study confirms a finite region of the RVB phase for the range of parameters $0.83(2) < v/t \leq 1$ [4, 33, 34, 35]. At $v/t = 0.83(2)$, the RVB phase undergoes a transition to a crystal phase, with the transition apparently of the second order [36, 35] (Fig. 4). At $v/t = 1$, a transition between the RVB phase and another crystal phase is of the first order.

Vortex-like excitations (visons)

The existence of the topological order on multiply-connected domains also implies a new type of vortex-like excitations. In the definition of the topological order, the contour is chosen to be either closed or connecting the edges of the domain. If now one takes a contour Γ connecting two points *inside* the lattice (connecting two plaquettes), then the operator of the parity of dimer intersections with such a contour no longer commutes with the Hamiltonian. In fact, one can show that this parity operator can be represented as a product of two point-like objects:

$$V_1 \cdot V_2 = (-1)^{N_\Gamma} \qquad (2)$$

where N_Γ is the number of the dimer intersections with the contour Γ. The operators V_1 and V_2 are associated with the end points of the contour, but they are nonlocal in terms of dimer operators. They produce a certain type of vortexlike excitations (dubbed visons) [27, 28]. While the operators V_1 and V_2 applied to the ground state do not produce an eigenstate, they may be dressed by local dimer operators and translated with a given wave vector to produce eigenstates of the Hamiltonian of the quantum

dimer model. The operators V_i have the structure of Z_2 vortices: they can only be created in pairs in a finite system, and a product of two such operators can be expressed locally in terms of dimer operators. So the true vison eigenstates are the lowest-energy states equivalent to the states V_i [37].

Note that the operators V_i are defined on the dual lattice (i.e., on the lattice formed by the plaquettes of the original lattice) with a frustration (so that the operator V_i acquires the sign -1 if moved around one site of the original lattice), Fig. 5. Equivalently, one may think of a particle on the dual lattice in the magnetic field of half flux quantum per plaquette of the dual lattice. This determines the symmetry of the vison excitations and the structure of its Brillouin zone.

Visons in the RK dimer model

Vison excitations have been studied numerically in the Rokhsar–Kivelson dimer model. The numerics is especially simple at the Rokhsar–Kivelson point (at $v = t$): in that case, one can use the equivalence between the quantum system in imaginary time and a classical stochastic process [15] and model the quantum dynamics with a classical Monte Carlo simulation. This approach has been implemented in the work [37], where the full dispersion of vison excitations has been obtained (except for the high-energy part of the branch, where the visons are unstable with respect to decay into triples of visons). The lowest energy of the vison excitations equals 0.089(1) (in the units of $v = t$), which is smaller than the lowest energy of excitations generated by dimer operators. It has been thus shown that visons constitute the elementary excitations in this RVB state.

The analysis of the vison spectrum has been later extended away from the RK point, to $v/t < 1$ (with a more complicated numerical technique) [35]. It has been found that the visons continue to be the lowest-energy excitations throughout the RVB phase, and that their energy decreases (and apparently goes to zero) at the crystallization phase transition around $v/t = 0.83(2)$, see Fig. 4. Thus the crystallization transition may be described as a second-order vison condensation, in agreement with the conjecture of Ref. [36].

RVB PHYSICS IN GUTZWILLER-PROJECTED WAVE FUNCTIONS

An interesting and not yet fully resolved question is to what extent the physics described above (topological order and vison excitations) survives if one goes back from dimer models to spin systems. One of the obstacles is the overlap between various dimer configurations and non-uniqueness of the decomposition of a spin state in terms of products of singlets. A promising way around this difficulty is to consider Gutzwiller-projected wave functions as prototype states with RVB structure.

The idea of the Gutzwiller-projected construction is the following [38]: First, one considers a mean-field BCS-type quadratic Hamiltonian $H_{\rm BCS}(\chi,\Delta)$ (where χ and Δ are the sets of hopping and pairing amplitudes, typically restricted to a certain symmetry class and involving only one or several nearest-neighbor types of bonds). Then the ground state $\Psi_{\rm BCS}$ of this Hamiltonian is projected onto the configurations with no double occupancy of sites. In addition, the total electron density is fixed either by projecting onto a fixed-electron-number sector or by adjusting a chemical-potential term. This procedure is called the Gutzwiller projection P_G. The resulting wave function $\Psi_{\rm GP} = P_G\Psi_{\rm BCS}$ is considered as a variational wave function for the physical Hamiltonian $H_{\rm phys}$. The variational parameters χ and Δ are then adjusted to minimize the variational energy $\langle\Psi_{\rm GP}|H_{\rm phys}|\Psi_{\rm GP}\rangle$.

This variational approach to strongly-correlated Hamiltonians $H_{\rm phys}$ has been widely used both for a variety of spin systems [39, 40, 41] and for the t–J model in the context of high-temperature superconductivity [17, 18, 21]. Not only provides it a good variational ansatz for such systems, but it also implies a RVB-type structure [2]. One is then tempted to ask whether the argument in Ref. [2] can be promoted to the topological order and visons, by analogy with the dimer models. Several developments have been made in this direction.

Topological order in projected wave functions

To test for topological order, one needs to verify the two conditions formulated above for the ground states in different topological sectors. Such states are constructed variationally by projecting fermionic states with either periodic or antiperiodic boundary conditions on multiply connected domains [29]. If one considers an undoped system (a spin model), such a projection produces the same spin boundary conditions, regardless of the choice of fermionic boundary conditions. One can then check whether the two criteria for the topological order are satisfied or not (both criteria become nontrivial in this case).

In Ref. [29], we have performed such a test for several types of wave functions similar to those used for the t–J model and for the J_1–J_2 spin model. We have found that some of them do not have a topological order, while some others do. Note that since the mean-field states

$\Psi_{\rm BCS}$ used in our study have nodes in the spectrum, the conditions for the topological order, even if they are satisfied, hold not with an exponential, but only with a power-law accuracy for large systems. For example, for the nearest-neighbor spin correlations we find

$$\langle +|S_i S_j|+\rangle - \langle -|S_i S_j|-\rangle \propto L^{-\alpha}\,, \quad \alpha \approx 2\,, \qquad (3)$$

where $|+\rangle$ and $|-\rangle$ are Gutzwiller-projected states with different fermionic boundary conditions, and L is the linear system size.

A similar numerical study has been performed later by another group [42] on a different set of wave functions. They have also observed that some of the projected wave functions possess a topological order while others don't. However the problem of finding the exact criteria on the wave function for the appearance of the topological order is not solved yet: in Ref. [29], we argue that it should be determined by whether the mean-field ansatz is of the Z_2 or of the $U(1)$ type, while in Ref. [42] they claim that it is the bipartite geometry of the lattice which is responsible for the presence or absence of topological order in the projected wave function. Neither of the two conjectures is solidly proven, and the collection of available numerical evidence collected in the two papers appear to be inconsistent with either of the two conjectures. Therefore it seems necessary to undertake either a more detailed and systematic numerical study of this problem or to present a rigorous analytic argument to resolve the issue of topological order in Gutzwiller-projected wave functions.

GENERALIZATION OF THE RVB CONSTRUCTION: LOOP PATH INTEGRAL

An interesting complication arising in the study of topological order in Gutzwiller-projected wave function is the presence of nodes in the mean-field state. Those nodes result in the *algebraic* topological order. Moreover, the original argument of Anderson about the RVB nature of Gutzwiller-projected wave functions [2] is not applicable to BCS states with nodes (since the resulting singlet amplitudes become long-ranged in this case). This issue has been addressed in Ref. [30], where the RVB structure of wave functions has been interpreted in terms of the loop path integral, instead of singlets.

The idea is to consider the "partition function" $\langle\Psi|\Psi\rangle$ instead of the wave function $|\Psi\rangle$. For all known examples of RVB states, this normalization of the wave function has the form

$$\langle\Psi|\Psi\rangle = \sum_{\{C_n\}} \prod_n A(C_n)\,, \qquad (4)$$

where the sum is taken over all possible fully packed coverings of the lattice by the loops C_n (so that every site belongs to exactly one loop), and $A(C_n)$ is some function of the loop. This construction obviously generalizes the expression for the overlap of the conventional RVB states (built as products of singlets [2]):

$$A(C) = -2a_{12}a_{23}\ldots a_{k1} \qquad (5)$$

where a_{ij} are the singlet amplitudes. The minus sign in the expression for $A(C)$ comes from the fermionic structure of the RVB construction (a positive sign would also be possible [43]), and the factor of 2 reflects the spin multiplicity. The loops are formed by the overlap of dimer singlets in the bra and ket vectors $\langle\Psi|$ and $|\Psi\rangle$ (Fig. 6).

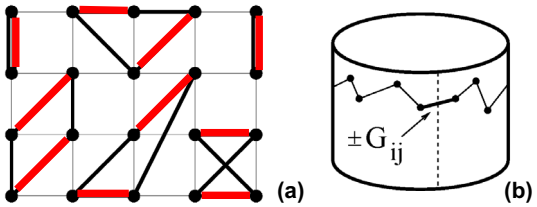

FIGURE 6. **(a)**: In the conventional RVB construction, the loops are given by the overlap of two singlet (dimer) configurations. **(b)**: The topological sectors may be accessed by changing the sign of the amplitude for loops having a global winding.

However, the loop-path-integral expression (4) has a wider range of validity: in fact, all known RVB-like states can be interpreted in this way. For example,

1. As mentioned above, the RVB state composed of products of singlets corresponds to the choice $A(C) = -2a_{12}a_{23}\ldots a_{k1}$.
2. The ground state of the Rokhsar–Kivelson dimer model at the RK point ($t = v$) corresponds to
$$A(C) = \begin{cases} 1 & \text{for length-two loops} \\ 0 & \text{otherwise} \end{cases} \qquad (6)$$
3. For Gutzwiller-projected wave functions [30],
$$A(C) = -\mathrm{Tr}\, G_{12}G_{23}\ldots G_{k1}\,, \qquad (7)$$
where G_{ij} are the BCS equal-time Green functions (2×2 matrices).

The last example is interesting from the point of view of the algebraic topological order. Indeed, the topological order may be formulated in terms of the loop behavior in the path-integral theory (4). Different topological sectors may be accessed by assigning a minus sign for globally winding loops (Fig. 6). The two conditions of topological order may be qualitatively formulated as (1) loops are short ranged and (2) loops do not crystallize [30]. The short-rangedness of loops is however only algebraic in the example of projected BCS states with nodes. In such

a case, since the Green functions G_{ij} decay algebraically (as L^{-2}), the loop size cannot decay faster than that (since there always exist "direct-flight" loops with long-range links), but can only decay equally fast or slower than G_{ij}. This imposes an upper bound on the convergence of the topological degeneracy for such projected states in the thermodynamic limit.

A more accurate analytic description of algebraic topological order in Gutzwiller-projected wave functions is still to be completed. Numerical studies indicate that the close-packing constraint strongly renormalizes the algebraic topological order, as compared to the power-law decay of the bare Green functions G_{ij} [30].

RVB STATE IN DOPED SYSTEMS

Finally, it is worth commenting on the fate of topological order and of vortex-like excitations in RVB systems doped with mobile charges (with high-temperature superconductivity in mind). A general theory of doped RVB states still needs to be completed, and a great part of research in high-temperature superconductivity is devoted to this direction.

One obvious scenario (supported by the study of Gutzwiller-projected wave functions) is that upon doping the system immediately becomes superconducting. In that case the vison excitations get promoted to superconducting vortices [29]. It has been even conjectured that vison excitations may survive above the superconducting transition temperature [28], but so far this conjecture has not found any experimental confirmation [44].

Another interesting question is the spin-charge separation in doped RVB systems. While the naïve picture predicts that the spin and charge excitations should be decoupled in a liquid of RVB dimers (see, e.g., a monomer-monomer correlation function acquiring a finite expectation value in the RK dimer model [31]), the Gutzwiller-projected construction of quasiparticles [22, 23, 24, 25, 45, 46] suggests that, to the contrary, the spin and charge are bound to form a renormalized BCS-like quasiparticle. A resolution of this apparent inconsistency may lie in the observation that the spectral weight of the quasiparticle goes to zero in the limit of zero doping [22]. Therefore, the spin and charge separated at half filling may gradually recombine upon doping. It may be interesting to find a model (possibly an extension of the RK model) where the problem of spin-charge recombination may be treated analytically, to give an insight in the physics of doped RVB systems.

ACKNOWLEDGMENTS

I am grateful to P. A. Lee, T. Senthil, M. Feigelman, A. Ioselevich, F. Mila, A. Ralko, F. Becca, and M. Ferrero for collaboration on different topics mentioned in this review. The work was supported by the Swiss National Foundation.

REFERENCES

1. C. Lhuillier and G. Misguich, in *High Magnetic Fields*, Lecture Notes in Physics **595** (Springer, Berlin, 2002); C. Lhuillier, cond-mat/0502464 and refs. therein.
2. P. W. Anderson, Science **235**, 1196 (1987).
3. G. Misguich et al, Phys. Rev. B **60**, 1064 (1999); R. Sindzingre, C. Lhuillier, and J.-B. Fouet, cond-mat/0110283; G. Misguich et al, Eur. Phys. J. B **26**, 167 (2002).
4. R. Moessner and S. L. Sondhi, Phys. Rev. Lett. **86**, 1881 (2001).
5. L. Balents, M. P. A. Fisher, and S. M. Girvin, Phys. Rev. B **65**, 224412 (2002).
6. T. Senthil and O. Motrunich, Phys. Rev. B **66**, 205104 (2002); O. Motrunich and T. Senthil, Phys. Rev. Lett. **89**, 277004 (2002).
7. G. Misguich, D. Serban, V. Pasquier, Phys. Rev. Lett. **89**, 137202 (2002).
8. L. B. Ioffe and M. V. Feigelman, Phys. Rev. B **66**, 224503 (2002).
9. J. S. Helton et al, Phys. Rev. Lett. **98**, 107204 (2007); P. Mendels et al, Phys. Rev. Lett. **98**, 077204 (2007); O. Ofer et al, arXiv:cond-mat/0610540 (2006).
10. P. Fazekas and P. W. Anderson, Philos. Mag. **30**, 423 (1974).
11. G. Misguich and C. Lhuillier, in *Frustrated spin systems*, ed. H. T. Diep (World-Scientific, Singapore 2005).
12. R. Moessner, S. L. Sondhi, and E. Fradkin, Phys. Rev. B **65**, 024504 (2002).
13. D. S. Rokhsar and S. A. Kivelson, Phys. Rev. Lett. **61**, 2376 (1988).
14. M. E. Fisher and J. Stephenson, Phys. Rev. **132**, 1411 (1963).
15. C. Henley, J. Phys. Condens. Matter **16**, S891 (2004); J. Stat. Phys. **89**, 483 (1997).
16. R. Moessner and S. L. Sondhi, Phys. Rev. Lett. **86**, 1881 (2001).
17. C. Gros, Phys. Rev. B **38**, 931 (1988); Ann. Phys. **189**, 53 (1989).
18. H. Yokoyama and H. Shiba, J. Phys. Soc. Jpn. **57**, 2482 (1988); H. Yokoyama and M. Ogata, J. Phys. Soc. Jpn. **65**, 3615 (1996).
19. A. Himeda and M. Ogata, Phys. Rev. B **60**, 9935 (1999).
20. D. A. Ivanov, Patrick A. Lee, and X.-G. Wen, Phys. Rev. Lett. **84**, 3958 (2000).
21. P. W. Anderson et al, J. Phys. Cond. Matt. **16**, R755 (2004).
22. A. Paramekanti, M. Randeria, and N. Trivedi, Phys. Rev. Lett. **87**, 217002 (2001), Phys. Rev. B **70**, 054504 (2004), Phys. Rev. B **69**, 144509 (2004).
23. K.-Y. Yang et al, Phys. Rev. B **73**, 224513 (2006).

24. H. Yang, F. Yang. Y.-J. Jiang, and T. Li, J. Phys.: Condens. Matter **19**, 016217 (2007).
25. C.-P. Chou, T. K. Lee, and C.-M. Ho, Phys. Rev. B **74**, 092503 (2006).
26. N. Read and B. Chakraborty, Phys. Rev. B **40**, 7133 (1989).
27. S. A. Kivelson, D. S. Rokhsar, and J. P. Sethna, Phys. Rev. B **35**, 8865 (1987).
28. T. Senthil and M. P. A. Fisher, Phys. Rev. B **62**, 7850 (2000); ibid. **63**, 134521 (2001).
29. D. A. Ivanov and T. Senthil, Phys. Rev. **B** 66, 115111 (2002).
30. D. A. Ivanov, Phys. Rev. B **74**, 024525 (2006).
31. P. Fendley, R. Moessner, and S. L. Sondhi, Phys. Rev. B **66**, 214513 (2002).
32. A. Ioselevich, D. A. Ivanov, and M. V. Feigelman, Phys. Rev. B **66**, 1744405 (2002).
33. A. Ralko, M. Ferrero, F. Becca, D. Ivanov, and F. Mila, Phys. Rev. B **71**, 224109 (2005).
34. A. Ralko, M. Ferrero, F. Becca, D. Ivanov, and F. Mila, Phys. Rev. B **74**, 134301 (2006).
35. A. Ralko, M. Ferrero, F. Becca, D. Ivanov, and F. Mila, Phys. Rev. B **76**, 140404(R) (2007).
36. R. Moessner and S. L. Sondhi, Phys. Rev. B **63**, 224401 (2001).
37. D. A. Ivanov, Phys. Rev. B **70**, 094430 (2004).
38. M. C. Gutzwiller, Phys. Rev. Lett. **10**, 159 (1963); Phys. Rev. A **134**, 1726 (1965).
39. D. V. Dmitriev, V. Ya. Krivnov, V. N. Likhachev, and A. A. Ovchinnikov, Fiz. Tv. Tela **38**, 397 (1996) [Phys. Solid State, **38**, 219 (1996)].
40. L. Capriotti, F. Becca, A. Parola, and S. Sorella, Phys. Rev. Lett. **87**, 097201 (2001).
41. Y. Ran, M. Hermele, P. A. Lee, and X. G. Wen, Phys. Rev. Lett. **98**, 117205 (2007).
42. T. Li and H.-Y. Yang, Phys. Rev. B **75**, 172502 (2007).
43. S. Liang, B. Douçot, and P. W. Anderson, Phys. Rev. Lett. **61**, 365 (1988).
44. D. A. Bonn et al, Nature **414**, 887 (2001); J. C. Wynn et al, Phys. Rev. Lett. **87**, 197002 (2001).
45. C. P. Nave, D. A. Ivanov, and P. A. Lee Phys. Rev. B **73**, 104502 (2006).
46. S. Bieri and D. Ivanov, Phys. Rev. B **75**, 35104 (2007).